arXiv:1209.0322v1 [astro-ph.SR] 3 Sep 2012

BAASP, 2012

ON THE VARIABILITY OF TOTAL SOLAR IRRADIANCE

J. Pelt and O. Kärner

Tartu Observatory, Tõravere, 61602, Estonia

Received: 2012 x x; accepted: xxxx x x

Knowing the variability of total solar irradiance (TSI) at the top of the atmosphere is crucial for specifying solar influence to climate variability. Satellite measured TSI data are available only for the last 32 years. But there is an opportunity to estimate approximate daily TSI values on the basis of the observed variability of solar activity. A common approach is based using data for Wolf sunspot numbers. Series of daily data from the DAVOS based TSI starting from 1978 have been compared with daily values of Wolf numbers and with the corresponding estimates for daily summary sunspot area. Our goal is to use established correlations to hindcast earlier TSI values. The available solar activity data enabled us to reproduce rough TSI estimates back to the 1870's.

Key words: astrophysics, climatology: observations – total solar irradiance, solar magnetic activity – methods: statistical

1. INTRODUCTION

Modern climatological thinking is based on the dominating role of the anthropogenic global warming theory (Solomon et al. 2007). It is supported by continuous increase of the concentration of carbon dioxide in the Earth's atmosphere. To estimate validity of that conception it is necessary to know the temporal variability of other forcing factors, among them the total solar irradiance (TSI) at the top of the atmosphere. Direct satellite measurements on that flux have been carried out only since 1978. But this flux density depends on solar magnetic activity describable by Wolf numbers or other indicators. Knowing the relationship between solar activity and TSI enables us to hindcast the TSI series more than 100 years back on the basis of observations of sunspots. This enables one to estimate changes in solar forcing in comparison with that caused by the increase of CO_2 concentration in the Earth's atmosphere.

Solar activity is often characterized by means of sunspot numbers (or Wolf numbers) The corresponding quantitative characteristic R_w is computed as $R_w = k(10g + s)$, where s is number of distinct spots (independent on their size); G is number of spot groups and k is a coefficient to reconcile data with different observation places and telescopes. The other activity indicator used in the current

study is a daily sunspot area A_S, also available from historical records.

A time series for daily R_w has been observed from 1870. Satellite based TSI observations started in 1978. Two types of observations have been carried out simultaneously during the last three decades. This enables us to to empirically estimate statistical relationship between daily values of R_w, A_S and TSI. Physical basis of that relationship has been explained recently (e.g. Foukal et al. 2006): *Brightening of the Sun with increasing sunspot number is explained by the existence of bright magnetic areas called faculae. Each such dark or bright structure contributes to a TSI variation equal to the product of its projected area and its photometric contrast relative to the adjacent, undisturbed photometric disc.*

Much higher contrast of the faculae causes increase of TSI. Thus an examination of statistical relationship between daily values of R_w, A_S and TSI is justified.

Several attempts to hindcast previous TSI values have been performed using different time intervals. Diagnosed associations between sources of contemporary irradiance variability and appropriate solar activity proxies that extend over longer time spans permit the irradiance reconstructions for some earlier period (e.g. Lean 1997, Wenzler et al. 2006, Balmaceda et al. 2007, Steinhilber et al. 2009, Krivova et al. 2010, Shapiro et al. 2011). New reconstructions of spectral irradiance are developed for time base starting from 1600 with absolute scales traceable to space based observations. For instance an updated solar irradiance reconstruction (Lean 2000) on annual resolution is available online (Lean 2004).

In this paper we compare two methods to hindcast TSI values for earlier than observed dates. The first method is rough and is based on regression analysis of TSI *versus* R_w. The second method is a new and uses daily sunspot areas and corresponding TSI values to build empirical model for relation between the two observed series. The model is based on the observation that solar magnetic activity *correlates* with low-frequency flow of the TSI and at the same time *anti-correlates* with high frequency features. Our empirical model contains free parameters but values for them can be obtained from fitting procedure itself. Thereby our method is essentially parameter free and differs from traditional methods where modelling is based on heavily parametrized physical models (see for instance Krivova et al. 2007).

2. DATA

For general overview of the available TSI data and processing methods see e.g. Domingo et al. 2009. The original TSI satellite observations are compiled into homogeneus data sets, often called composites (for recent overviews and compiling methods see Ball et al. 2012 and Domingo et al. 2009). Results for daily TSI in Wm^{-2} for the time interval 1978.88-2012.02 have been downloaded from the website belonging to Davos Physical-Meteorological Observatory (PMOD)[1] (see Fröhlich and Lean 1998 for details and for updates Fröhlich 2006). All together there is 11428 adjusted measurements in composite data. The observation archives from Belgian Royal Observatory were used to download daily sunspot numbers[2] from 1818.02 to 2012.16 - all togeteher 67670 estimates. Sunspot daily areas were downloaded from NASA/Marshall Space Flight Center Solar Physics web pages[3].

[1] `ftp://ftp.pmodwrc.ch/pub/data/irradiance/composite`

[2] `http://www.sidc.be/DATA/dayssn_import.dat`

[3] `http://solarscience.msfc.nasa.gov/greenwch/daily_area.txt`

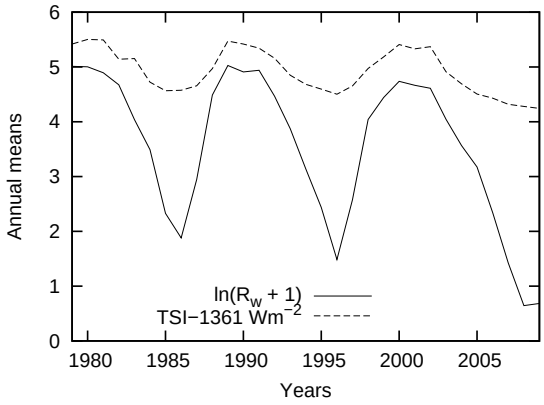

Figure 1: Comparison of the annual mean values for ln(R_w +1.) TSI anomalies i.e. $(TSI - 1361)$ in Wm^{-2} during the last 30 years.

This data set contains 50212 measurements from 1874.35 to 2012.16.

3. PRELIMINARY ANALYSIS

Annual mean values over the period from 16.11.1978 to 20.09.2010 have been computed for the comparison. The results are shown in Figure 1. In order to convert the draft better comparable, the R_w values are presented via logarithm i.e. ln(R_w+1.) and TSI data as difference from the constant 1361 Wm^{-2}.

Three important details can be found:

1. The both variables change in the same phase.
2. There is a remarkable difference in the length of the low activity periods.
3. The difference of TSI values between high and low activity seasons is in between $0.5 - 1$ Wm^{-2}.

The website `gaw.kishou.go.jp/wdcgg.html` for the World Database for Greenhouse Gases (WDCGG) states that the concentration of CO_2 grows at constant rate 1.6 ppm/year. Radiative transfer calculations (e.g. Schwartz 2007) have shown that the direct influence of doubling the concentration (i.e. from 320 ppm to 640 ppm) to the outgoing longwave radiation (OLR) flux density is about 4 Wm^{-2}. Provided that the growth rate does not change, it will take about $320/1.6 = 200$ years until the concentration doubles. This means that the annual part in the OLR flux growth is about $4/200 = 0.02$ Wm^{-2}. This value is significantly lower than the difference between TSI between high and low solar activity. The variability of TSI can in a such way dominate. However, its influence to the Earth climate remains dependent on cumulative feedback in the climate system.

4. APPROXIMATE DEPENDENCE of TSI on R_w

The existing dataset enables us to display approximate dependence of TSI on R_w. First, it is interesting to select spot free days. During the solar minimum of

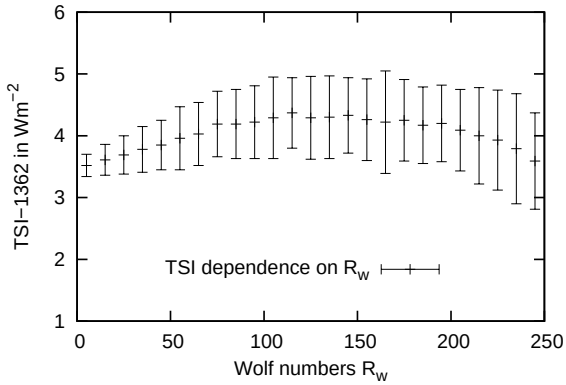

Figure 2: Range of daily variability for $TSI - 1362$ depending on different level of R_w. The days corresponding to $R_w = 0$ are excluded

2008, the value of TSI was more than 0.2 Wm^{-2} lower than during the previous minimum in 1996, indicating for the first time a directly observed long-term change (Fröhlich 2009). Direct comparison shows that the same difference occurs between the mean values for sunspot free days for the periods 1978-1999 and 2000-2010, respectively. Thus, for more accurate restoration we compare the daily R_w and TSI values over the period 1978-2003 only.

Empirical dependence of TSI on $R_w > 0$ is simple to figure out. In this case the region of variation (1 - 250) for R_w is partioned to 10 unit bins. As a result 25 bins are selected. Values of daily TSI (on the basis of PMOD composite) for each bin have been collected and their range is shown in Figure 2 with error bars. The mean TSI values of bins are marked by straight lines.

Figure 2 shows that the dependence of TSI on R_w is similar to the the arc produced by Solanki and Fligge (1999) and Hempelmann and Weber (2011). The latter study has been produced using ACRIM based TSI series. This is expected because both TSI series have been composed from measurements of the same satellites.

Maximal values of TSI correspond to R_w from the interval $100 < R_w < 150$. It appears to be somewhat more elaborate than a linear expectation on proportionality between spots and faculi could produce. Thus, the oscillation of R_w in between 0 and 250 causes an oscillation of TSI around somewhat higher level than that corresponding to TSI from a spotless Sun. Anyway, the increase of TSI as R_w is growing will be bounded. Approximate relationship between TSI and R_w shown in Figure 2 enables us to estimate TSI variability caused by the variations of solar activity. In the current case a restoration is carried out using the mean TSI values for each R_w interval presented in Figure 2 . The results will be presented together with those for the other method in Figure 8.

6. REFINED ANALYSIS USING A_S

Rough analysis done so far can be refined significantly. It is possible to build,

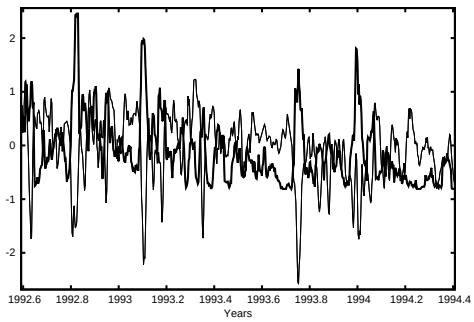

Figure 3: Comparison of the normalised TSI (thin line) and sunspot area values (thick line). The smaller details in the curves tend to anti-correlate.

based on various physical assumptions, so called model or proxy curves (see e.g. Krivova et al. 2007) and use them to hindcast daily TSI values. This kind of methods demand complicated physical modelling for different magnetic structures on the surface of the Sun (spots, penumbrae, flares and network). In this paper we try to hindcast using another parameter free scheme. In the following a more detailed dataset of sunspot areas A_S will be used instead of sunspot numbers.

It is well known that overall (low frequency) TSI flow quite well correlates with solar magnetic activity. But if to look at Figure 3 then it can be easily seen that the smaller details anti-correlate. This can be easily explained referring to darker sunspots moving on the surface of the Sun. From the point of view of the time series analysis such combination of varying correlation introduces extra complications. We need to model separately low frequency and high frequency parts of the input curves because of that difference.

6.1. Envelopes

Typically low frequency (smooth) components of the time series are obtained with different averaging and smoothing algorithms. In this work we used so called LOWESS (locally weighted scatterplot smoothing, see Cleveland 1979) method with linear downweighting to compute low frequency components. This method is constrained with only single parameter - a smoothing window width W. By changing this parameter it is possible to obtain curves with different degrees of smoothness.

The activity records of the Sun tend to be one sided. For instance sunspot areas are positive or zero. This forces us to consider additional time series component types beside the trivial smoothed or averaged data. The method to build such an one sided smooth curves has been employed earlier for processing of spectral data where the absorption or emission lines are superposed on a smooth continuum (e.g. Pelt 1990). This is very similar to the situation with sunspot blocking.

In our method the smoothing and one side clipping is performed iteratively to obtain a smoothed component which envelopes the input time series. In the very end of the iterations the smooth envelope goes through the local minima or maxima. We do not need perform all the iteration but can stop earlier, say at iteration K. Taking into account that smoothing operation itself depends on

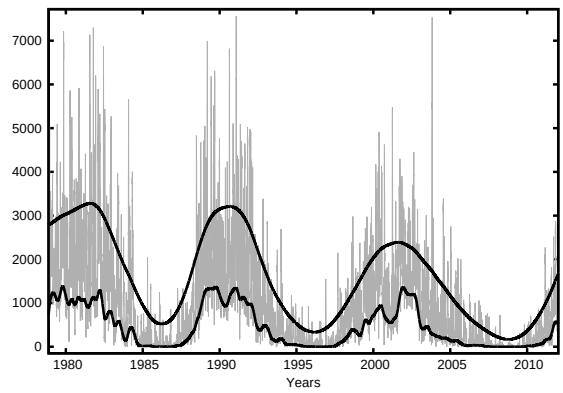

Figure 4: Original sunspot area data in millionth parts of solar surface, upper envelope $E^U(3.0, 4, t)$ and lower envelope $E^L(0.4, 9, t)$ for the sunspot areas. In this time interval we can use the enevelopes as fit components to model TSI.

the width parameter W we can formally build from input time series two sets of envelopes: $E^U(W^U, K^U, t)$ and $E^L(W^L, K^L, t)$. The first set describes upper part of the data and the second set lower part. An illustration of the envelopes is provided on Figure 4.

6.2. Regression

The least squares distance D^2 between four plus four parameter model buildt from sunspot area data ($S(t)$) and TSI ($I(t)$):

$$D^2 = \left(a_0 + a_1 E^L(W^L, K^L, t) + a_2 E^U(W^U, K^U, t) + a_3 S(t) - I(t)\right)^2 \qquad (1)$$

must be minimized to obtain proper estimates for the regression coefficents a_0, a_1, a_2, a_3 and also for smoothing parameters W^U,K^U,W^L and K^L. Combining linear least squares estimation with grid search for nonlinear parameters allows us to obtain final solution. The results for our particular case (daily values of PMOD composite for TSI *versus* records of sunspot areas) can be illustrated in different ways. First we can plot the difference between actual TSI and computed from sunspot areas TSI (see Figure 5). This plot can be compared with similar figure 4c from Krivova et al. (2007) where overall scatter of the differences between observed and predicted curves is somewhat higher.

The cross plot between the original and restored TSI values is presented on Figure 6. There is still considerable scatter but the correlation level between two series is quite high ($r = 0.826$). As a matter of fact this value is comparable to the scatter between different TSI composites (correlation between ACRIM and PMOD composites is at level $r = 0.834$).

In our earlier observation we saw that small details in the flow of the sunspot area data are anti-correlated with small details of the TSI flow. However, the weighted combination of sunspot area data and its envelopes shows much better correlation. This is a result of estimated a_3 value being less than zero. Positive

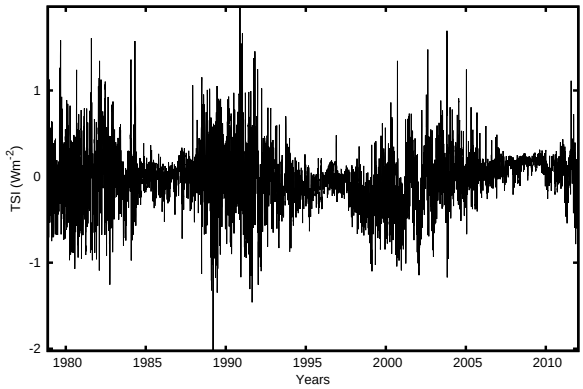

Figure 5: Comparison of the observed *versus* restored TSI values

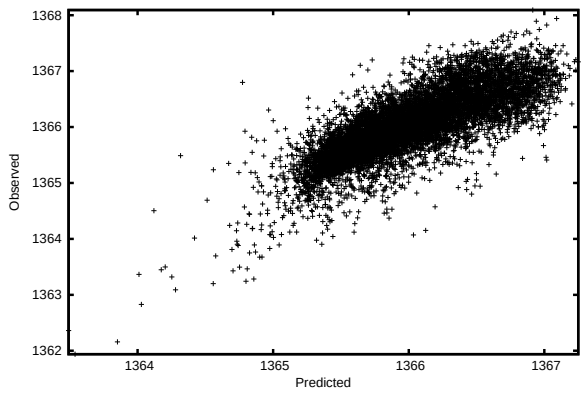

Figure 6: Scatter plot of the observed *versus* restored daily TSI values.

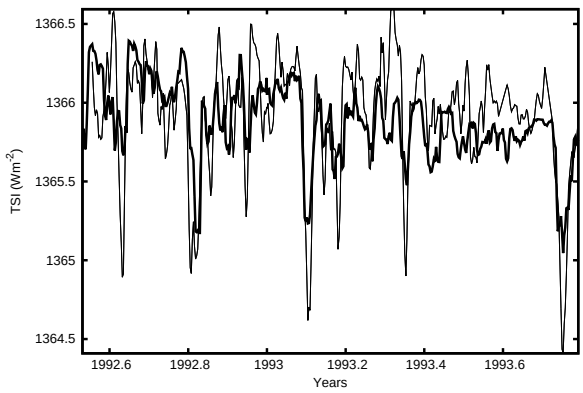

Figure 7: Small details and larger features of the estimated and original curve are now correlated.

correlation of the large scale features comes from contributions of envelope components $E^L(W^L, K^L, t)$ and $E^U(W^U, K^U, t)$. The situation is precisely illustrated on Figure 7.

Finally, it is useful to illustrate the results of restoration of TSI over our testing interval. The illustration is shown in Figure 8 in annual means of (TSI-1362) Wm^{-2}.

Figure 8 shows that the rough restoring operation has varying accuracy. For the regions of low solar activity its behavior is acceptable. But for the regions with high solar activity it gives a significant bias. This means that it is not applicable to use the scheme to hindcast previous TSI values. The second method (even after averaging) gives much better accordance with the original values over that interval.

The hindcasted daily values of TSI for the whole time interval with available A_S data is presented at Figure 9. This series can be used in modelling programs or compared with temperature curves.

7. CONCLUSIONS

Hindcasting the previous TSI data is important in order to improve our understanding of climate variability. In this paper we used two methods to hindcast past TSI values using indicators of the solar magnetic activity as a base. The rough and more traditional regression method was supplanted by the refined method which uses daily values of the sunspot areas. The refined method is essentially parameter free. This is important because the traditional hindcast methods are based on a large set of parametric physical models of the solar features. Here we demonstrate that the low frequency behaviour of the TSI is controlled by the low frequency components of the magnetic activity. However, this dependence is not straight forward but somewhat convoluted. Similar result was obtained by using signal theory methods of empirical data modelling (Preminger 2010). The obvious advantage of proposed here method is its conceptual transparency - upper and lower envelopes are easily grasped and visualized. We plan to use the new method

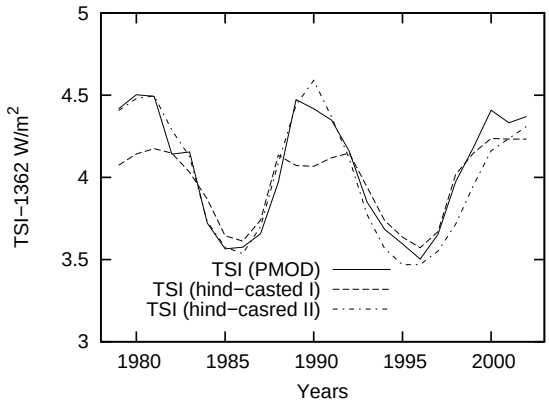

Figure 8: Comparison of the measured annual mean TSI_{PMOD} values with the annual mean values computed using the two hindcasting schemes, respectively.

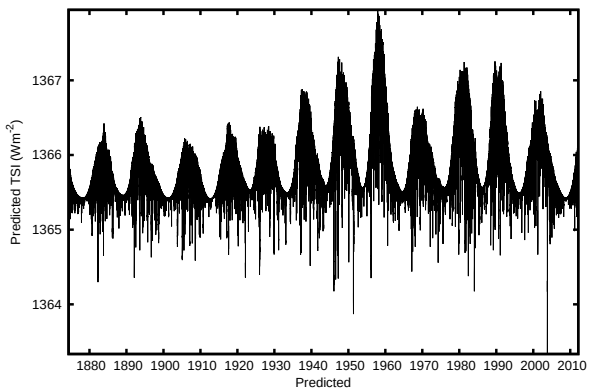

Figure 9: The TSI values for previous years computed from the daily sunspot areas.

in different contexts.

Variability of the hindcasted TSI values shows that the interannual variability of TSI has been nearly of the same range as that during the last three decades. Previous studies have shown a remarkable variability of the solar cycle length to influence the long-term variability in the climate system (e.g. Lassen and Friis-Christensen 1995). The described empirical relationship between TSI and solar activity enables one to examine such an influence in more detail.

REFERENCES

Ball W.T, Unruh Y.C., Krivova N.A. et al. (2012). Reconstruction of total solar irradiance 1974 - 2009. *arXiv:1202.3354v1*,1-15.

Balmaceda L., Krivova N.A., Solanki S.K. (2007). Reconstruction of solar irradiance using the Group sunspot number, *Adv. Space Res., 40*, 986989.

Barnhart B.L., Eichinger W.E. (2011). Empirical Mode Decomposition applied to solar irradiance, global temperature,sunspot number,and CO^2 concentration data, *Journ. Atmos. Solar-Terr. Phys, 73*, 1771-1779.

Cleveland W.S. (1979). Robust Locally Weighted Regression and Smoothing Scatterplots *J. Amer. Stat. Assoc., 74*, 829836.

Domingo V., Ermolli I., Fox P. et al. (2009). Solar Surface Magnetism and Irradiance on Time Scales from Days to the 11-Year Cycle, *Space Sci. Rev.,145*,337-380.

Foukal P., Frölich C., Spruit H., Wigley T.M.L., (2006). Variations in solar luminosity and their effect on the Earth's climate. *Nature, 443*, 161-166.

Fröhlich C. (2009). Evidence of a long-termtrend in total solar irradiance. *Astron. and Astrophy., 501*,L27-L30. DOI: 10.1051/0004-6361/200912318.

Fröhlich C., Lean J. (1998). The Suns Total Irradiance: Cycles and Trends in the past two decades and associated Climate Change Uncertainties. *Geophys.Res.Lett., 25*, 4377-4380.

Fröhlich, C., (2006). Solar irradiance variability since 1978: Revision of the PMOD composite during solar cycle 21, *Space Sci. Res., 125*, 5365.

Hempelman A., W. Weber (2011). Correlation between the sunspot number, the total solar irradiance, and the terrestrial insolation. *Solar Phys., 277*, 417-430, DOI 10.1007/s11207-011-9905-4.

Krivova N.A., Balmaceda L., Solanki S.K. (2007). Reconstruction of solar total irradiance since 1700 from the surface magnetic flux, *Astron. and Astroph., 467*, 335-346.

Krivova N.A., Vieira E.A., Solanki S.K. (2011). Reconstruction of solar spectral irradiance since the Maunder minimum, *J. Geophys Res., 115*, A12112,1-11.

Lassen K., Friis-Christensen E. (1995). Variability of the solar cycle length during the past five centuries and the apparent association with terrestrial climate. *J. Atmos. Solar.-Terr. Phys., 57*, 835-845.

Lean J. (1997). The Sun's variable radiation and its relevance for earth. *Rev. Astron. Astrophys., 35*, 33-67.

Lean J. (2000). Evolution of the Sun's Spectral Irradiance Since the Maunder Minimum. *Geophys. Res. Lett., 27*,2425-2428.

Lean J. (2004). Irradiance Reconstruction. *IGBP PAGES/World Data Center for Paleoclimatology. Data Contribution Series No 2004-035.* NOAA/NGDC Paleoclimatology Program, Boulder, CO, USA.

Pelt J. (1990). A Method of Continuum Estimation in Spectral Classification Experiments, *Bulletin d'Information du Centre de Donnees Stellaires*, 38, 95-

107.

Preminger D., Nandy D., Chapman G., Martens P.C.H (2010). Empirical Modeling of Radiative versus Magnetic Flux for the Sun-as-a-Star. *Solar Physics, 264*, 13-30.

Schwartz S.E. (2007). Heat capacity, time constant, and sensitivity of Earth's climate system. *J. Geophys. Res., 112, D24S05*,1-12.

Solomon S., Qin S., Manning M. et al. eds. (2007). *Climate Change, The Physical Science basis*, Cambridge University Press.

Shapiro A.I., Schmutz W., Rozanov E., Schoell M., Haberreiter M., Shapiro A.V., Nyeki S. (2012). A new approach to the long-term reconstruction of the solar irradiance leads to large historical solar forcing, *Astron. and Astrophys., 529*, A67, 1-8.

Solanki S.K., M. Fligge (1999). A reconstruction of total solar irradiance since 1700. *Geophys. Res. Lett., 26*, 2465-2468.

Steinhilber F., Beer J., Fröhlich C. (2009). Total solar irradiance during the Holocene, *Geophys. Res. Lett., 36*, L19704,1-5.

Wenzler T., Solanki S.K., Krivova N.A., Fröhlich C. (2006). Reconstruction of solar irradiance variations in cycles 21-23 based on surface magnetic fields *Astron. and Astrophys. 460*, 583 -595